AIAA 2000-3919

Experimental Investigation of Airfoil Drag Measurement With Simulated Leading-Edge Ice Using the Wake Survey Method

Biao Lu and Michael B. Bragg
University of Illinois at Urbana-Champaign
Urbana, IL

18th AIAA Applied Aerodynamics Conference and Exhibit
14–17 August 2000
Denver, Colorado

EXPERIMENTAL INVESTIGATION OF AIRFOIL DRAG MEASUREMENT WITH SIMULATED LEADING-EDGE ICE USING THE WAKE SURVEY METHOD

Biao Lu*
Michael B. Bragg†

University of Illinois at Urbana-Champaign

ABSTRACT

This paper describes a study of the wake survey method for drag measurement for bodies with large unsteady separated wakes. The intended application is airfoil testing with simulated ice accretions. Detailed surveys of the wakes of an S809 18"-chord airfoil, with and without simulated ice, and a 1" diameter cylinder were acquired. In the investigation, a 7-hole probe, a Pitot total-pressure probe, a $\cos^2$ probe, and a single element hot-wire probe were used to measure total and static pressures, all three components of wake velocity and the turbulence intensity. The effect of the type of probe on the pressure measurement in the turbulent flow was analyzed. The Jones' formula and van Dam's equation, which includes the effect of the Reynolds stress, were used in the calculation of the profile drag coefficient. The results showed a significant effect of wake turbulence on the pressure probe measurements and the calculated drag coefficient when the turbulence intensity was greater than 8 percent. The drag coefficient results from the 3 different probes and the two wake drag equations could be brought into reasonable agreement by correcting the data based on the measured wake turbulence.

NOMENCLATURE

AoA	Angle of attack
c	Chord of the airfoil
C_d	Drag coefficient
D	Drag, or Diameter of the cylinder
$\vec{F}$	Force vector
L	Characteristic length of the model
$\vec{n}$	Surface outer normal vector
p_t	Total pressure
p_s	Static pressure
q	Dynamic pressure, $\frac{1}{2}\rho V^2$
Re	Reynolds number
U	Freestream velocity
$\vec{V}$	Velocity vector
u, v, w	Velocity components in x, y and z direction, respectively
u', v', w'	Components of the fluctuation of velocity
x, y, z	Cartesian coordinates

Symbols:

α, β	Flow angles
ρ	Density of air
μ	Absolute viscosity of air,

Subscripts:

∞	Freestream value
w	Value in the wake
rms	Root mean square value
x, y, z	Value in x, y or z direction

INTRODUCTION

The total drag of an airfoil is usually determined by either force-balance measurements or the wake survey technique. Compared to the force-balance method, the wake survey method has the advantage that flow diagnostic information and, in 3-D flow, the profile and induced drag coefficient components can be obtained.

For the 2-D problem, the equations derived by Betz[1] and Jones[2] are usually used to calculate profile drag. It has been shown that in the usual case there is no significant difference (<1%) between the drags

* Graduate Research Assistant, Department of Aeronautical and Astronautical Engineering, Member AIAA.
† Professor and Head, Department of Aeronautical and Astronautical Engineering, Associate Fellow AIAA.

determined by the Betz and the simplified Jones equations.[3,4]

Takahashi[3] has shown that wake survey methods have problems dealing with separated flow. Current wake survey methods were derived based on the assumption that the flow at the wake survey station is steady. So the wake survey method is known to have limitations when investigating unsteady, highly turbulent wakes that occur for highly separated flows. This often occurs when measuring the drag on an airfoil with a simulated ice accretion. In order to study the effect of separated and highly turbulent flow on the calculation of drag coefficient, a 1" diameter cylinder was used in the investigation.

Antonia and Rajagopalan,[5] Chao and van Dam[6] and van Dam[7] derived the wake drag integral equations including the effects of turbulence. These equations include the axial component of turbulence and require that it be measured or estimated.

Turbulence also effects the measurement of the total and static pressures. Total pressure probes aligned with the mean flow direction read increased total pressure due to the effect of the turbulent velocity components in axial and the cross-stream plane. Goldstein[8] first quantified these effects. Becker and Brown[9] obtained an empirical fit to the response of various total pressure probe designs to a steady-state flow angularity. Rossow[10,11] also analyzed the turbulence effects on both total and static pressure probes and designed probes to eliminate or reduce the effects of the cross-stream turbulence.

Some assumptions were made based on the results of Coles and Wadcock[12] and Cantwell and Coles[13] to correct the readings of the probes used in this paper. Coles and Wadcock[12] investigated the flow past an NACA 4412 airfoil at maximum lift by using an X-array flying hotwire. The Reynolds number based on chord was about 1.5×10^6. It was found that the maximum u_{rms}^2/U_∞^2 and w_{rms}^2/U_∞^2 were around 0.08 and 0.05 respectively at the location of 0.14c downstream from the trailing edge according to the contours presented in their paper[12]. They also showed that the maximum u_{rms}^2/U_∞^2 and w_{rms}^2/U_∞^2 were around 0.01 and almost equal at the 0.8c downstream location.

The same X-array flying hotwire was also used in Cantwell and Coles[13] test to investigate the turbulence characteristics of the wake of a 10.14 cm diameter stainless-steel cylinder with a 2.97 m length. The Reynolds number based on diameter was 1.4×10^5. According to the contours they presented, it can be found that the maximum u_{rms}^2/U_∞^2 and w_{rms}^2/U_∞^2 were about 0.045 and 0.052, respectively. This was located at the center of the wake 8-diameters downstream and tended to be equal as the distance to the center of the cylinder increased. Cantwell and Coles[13] also found that the drag coefficient of the cylinder was 1.237 in the range of Reynolds number from 69,000 to 140,000 based on surface pressure integration.

The main objective of this work was to develop a practical and accurate wake survey technique for investigating unsteady wakes generated from airfoils with ice accretions. First, the integral equations for determining drag coefficient from wake measurements are presented. Then, the effect of turbulence on pressure probes is briefly discussed. Finally results from the test of a circular cylinder and a S809 airfoil are presented and the effect of the wake turbulence discussed.

WAKE SURVEY METHODS

Wake-Survey Equations

The equations used for calculating the drag can be derived from a simple aerodynamic analysis by application of the conservation law of momentum and mass to the control volume enclosing the object as shown in Fig.1.

According to van Dam's analysis[6,7] the linear momentum relation for the fixed control volume, V, enclosing the body in a steady uniform oncoming flow with velocity of U_∞ is

$$\sum \vec{F} = \iint_S \rho \vec{V}\left(\vec{V}\cdot\vec{n}\right)dS \qquad (1)$$

where $\sum \vec{F}$ is the vector summation of all forces acting on the fluid inside the control volume, ρ is the local mean flow density, $\vec{V} = u\hat{i} + v\hat{j} + w\hat{k}$ is the local mean flow velocity, $\vec{n} = n_x\hat{i} + n_y\hat{j} + n_z\hat{k}$ is the outward pointing unit vector normal to S, the closed control surface.

Neglecting the body force, the $\sum \vec{F}$ can also be expressed by the force generated by the body on the fluid, $-\vec{F}_b$, which is the drag, the pressure force on the fluid at S and the viscous force, τ, on the fluid at S. $\vec{F}$ can then be written as

$$\sum \vec{F} = -\vec{F}_b + \iint_S -p\vec{n}dS + \iint_S \tau : \vec{n}dS \qquad (2)$$

By combining the two equations above and taking the component in the streamwise direction, the drag can be expressed as

$$D = -\iint_S p n_x dS - \iint_S \rho u\left(\vec{V}\cdot\vec{n}\right)dS + \\ + \iint_S \left(\tau_{xx}n_x + \tau_{xy}n_y + \tau_{xz}n_z\right)dS \qquad (3)$$

Assuming the inlet and sides of the control surface are far away from the body and the flow is undisturbed at these locations, the expression for drag is

$$D = -\iint_{S_{exit}} \left(p_s - p_{s,\infty}\right)dS \\ - \iint_{S_{exit}} \left(\rho u^2 - \rho_\infty {U_\infty}^2\right)dS + \iint_{S_{exit}} \tau_{xx}dS \qquad (4)$$

By applying mass conservation,

$$\iint_{S_{exit}} (\rho u - \rho_\infty U_\infty)dS = 0$$

and assuming ρ is constant, the equation above becomes

$$D = -\iint_{S_{exit}} \left(p_s - p_{s,\infty}\right)dS \\ - \iint_{S_{exit}} \rho u\left(u - U_\infty\right)dS + \iint_{S_{exit}} \tau_{xx}dS \qquad (5)$$

According to Schlichting[14] and assuming the density is constant, the viscous stress, τ_{xx}, can be expressed as:

$$\tau_{xx} = 2\mu\frac{\partial u}{\partial x} - \rho\overline{u'^2} \qquad (6)$$

By assuming that the viscous component ($2\mu\frac{\partial u}{\partial x}$) is much smaller than the Reynolds stress component ($\rho\overline{u'^2}$) and can be neglected for high-Reynolds number flow, Eq. (5) can be simplified and written as

$$D = -\iint_{S_{exit}} \left(p_s - p_{s,\infty}\right)dS \\ + \iint_{S_{exit}} \rho u\left(U_\infty - u\right)dS - \iint_{S_{exit}} \rho\overline{u'^2}dS \qquad (7)$$

Since $D = \frac{1}{2}\rho {U_\infty}^2 L C_d$, where L is the characteristic length and C_d is the drag coefficient. Then the drag coefficient, C_d, can be expressed as

$$C_d = \iint_{S_{exit}} \left(\frac{p_{s,\infty} - p_s}{q_\infty}\right)d\left(\frac{S}{L}\right) \\ + 2\iint_{S_{exit}} \frac{u}{U_\infty}\left(1 - \frac{u}{U_\infty}\right)d\left(\frac{S}{L}\right) - 2\iint_{S_{exit}} \frac{\overline{u'^2}}{{U_\infty}^2}d\left(\frac{S}{L}\right)$$

Since $p_s = p_{s,\infty}$, $u = U_\infty$ and u' is very small and can be neglected outside the wake, and also assuming that the flow is uniform along spanwise, y direction, the equation above can be rewritten as

$$C_d = \int \left(\frac{p_{s,\infty} - p_{s,w}}{q_\infty}\right)d\left(\frac{z}{L}\right) \\ + 2\int \frac{u}{U_\infty}\left(1 - \frac{u}{U_\infty}\right)d\left(\frac{z}{L}\right) - 2\int \frac{\overline{u'^2}}{{U_\infty}^2}d\left(\frac{z}{L}\right) \qquad (8)$$

Theoretically this equation can be used at any downstream location for S_{exit}. However, the assumption simplifying the calculation of the viscous stress, τ_{xx}, is questionable when the integral plane S_{exit} is not far enough downstream of the body.

It can be seen from Eq.(8) that the total drag coefficient can be considered as the sum of the three components:

1) Pressure term: $\frac{2}{\rho {U_\infty}^2}\int \left(p_{s,\infty} - p_{s,w}\right)d\left(\frac{z}{L}\right)$

2) Momentum term: $2\int \frac{u}{U_\infty}\left(1 - \frac{u}{U_\infty}\right)d\left(\frac{z}{L}\right)$

3) Reynolds stress term: $-2\int \frac{\overline{u'^2}}{{U_\infty}^2}d\left(\frac{z}{L}\right)$

If the survey plane, S_{exit}, is far downstream of the body, it is reasonable to assume that $p_{s,w} = p_{s,\infty}$ and $\tau_{xx} = 0$, then the Eq.(5) becomes

$$D = \iint_{S_{exit}} \rho u\left(u - U_\infty\right)dS \qquad (9)$$

which is the starting point of Jones' derivation.[2] Following the Jones' derivation and assumptions, the drag coefficient can be expressed as

$$C_d = 2\int\sqrt{\frac{p_{t,w}-p_{s,w}}{q_\infty}}\left(1-\sqrt{\frac{p_{t,w}-p_{s,\infty}}{q_\infty}}\right)d\left(\frac{z}{L}\right) \quad (10)$$

By assuming $p_{s,w} = p_{s,\infty}$ in Eq. (10), the simplified Jones' equation can be found as

$$C_d = 2\int\sqrt{\frac{p_{t,w}-p_{s,\infty}}{q_\infty}}\left(1-\sqrt{\frac{p_{t,w}-p_{s,\infty}}{q_\infty}}\right)d\left(\frac{z}{L}\right) \quad (11)$$

Eqs. (8), (10), and (11) will be used in the Results and Discussion Section to calculate C_d for various cylinder and airfoil cases.

Pressure Measurement in a Turbulent Wake

The effect of turbulence on the measurement of both total and static pressure were first quantified by Goldstein.[8] According to his analysis with the assumption that the probe has equal sensitivity in the x, y and z directions, the expression for the measured (effective) total pressure can be expressed as

$$\begin{aligned} p_{t,eff.} &= p_s + \frac{1}{2}\rho u^2 + \frac{1}{2}K_t\rho\left(\overline{u'^2}+\overline{v'^2}+\overline{w'^2}\right) \\ &= p_{t,true} + \frac{1}{2}K_t\rho\left(\overline{u'^2}+\overline{v'^2}+\overline{w'^2}\right) \end{aligned} \quad (12)$$

where K_t is a constant and depended on the shape of the probe tip. This means that the probe is sensing a portion of the axial and crossflow turbulent energy as additional total pressure. The total pressure that is required in the drag equations is the true x-component of total pressure, $p_{t,true}$.

Rossow[10] analyzed the effect of turbulence on the readings of probes with different tip geometries and presented expressions for the measured total pressure. He stated that, for the chamfered Pitot tube, Fig. 2, the measured (effective) total pressure can be expressed as

$$p_{t,eff} = p_{t,true} + \frac{1}{2}\rho\left(\overline{u'^2}+\overline{v'^2}+\overline{w'^2}\right) \quad (13)$$

He also presented a probe design (Fig.2, $\cos^2$ probe) that has a steady-state response to flow angularity exactly as the cosine squared of the flow angle. For these probes, referred to as $\cos^2$ or Rossow probes, and the 7-hole probe, the measured (effective) total pressure is

$$p_{t,eff} = p_{t,true} + \frac{1}{2}\rho\overline{u'^2} \quad (14)$$

For probes with other tip geometries, if assuming the probe has the same sensitivity in both the y and z directions, the effective total pressure can be expressed as

$$p_{t,eff} = p_{t,true} + \frac{1}{2}\rho\overline{u'^2} + W_x\left(\frac{1}{2}\rho\overline{v'^2}+\frac{1}{2}\rho\overline{w'^2}\right) \quad (15)$$

Here W_x is the coefficient representing the sensitivity of the probe to the flow angularity and $W_x = 0$ indicates that the probe has the cosine squared characteristics as shown by Rossow.[10] If $W_x = 1$, Eq.(15) becomes the expression for the chamfered probe which is not sensitive to the flow angularity.

According to Goldstein's[8] analysis, if the probe has the same sensitivity in x, y and z direction, the measured static pressure (effective static pressure) can be express as

$$p_{s,eff.} = p_{s,true} + \frac{1}{2}\rho K_s\left(\overline{u'^2}+\overline{v'^2}+\overline{w'^2}\right) \quad (16)$$

where K_s is a constant to be determined by experiment. Goldstein[8] also stated that it probably lies between 0 and 2/3, and may depend on the size of the tube and on the arrangement of the holes.

It can be seen that, if the RMS of the three turbulence components, u', v' and w', can be determined by a hotwire or other sensor, and the characteristics of the probe are known, the 'true' total and static pressure can be obtained by subtracting turbulent dynamic pressure from the probe measurements.

Flow Angularity

Since the drag coefficient equation was derived based on the x-direction momentum analysis, the total pressure in x-direction, instead of the resultant total pressure should be used in the equation for calculating the drag coefficient. The total pressure due to flow in the x-direction, $p_{t,x}$, can be express as a function of the resultant total pressure, p_t, as the following equation

$$p_{t,x} = p_t\left(\cos\alpha\cos\beta\right)^2 \quad (17)$$

The flow angles α and β are defined in Fig. 3. For example, if $\alpha = \beta = 3°$, $p_{t,x} = 0.995p_t$. Therefore, for small flow angles the error is small.

Experimental Method

The test was performed in the Illinois 3 by 4ft low-speed wind tunnel. In the test, a 1" diameter cylinder and an S809 18"-chord airfoil, with and without simulated ice, were used, Fig. 4. The S809 airfoil is a modified version of the LS(1)-0417 for wind turbines. A quarter-inch, quarter-round ice shape, shown in Fig.4, was attached on the upper surface at the 10% surface chord location to simulate the ice accretion.

The survey plane, a cross-stream plane in which the probe measurements were taken is shown in Fig. 5. For the S809 the survey plane was 30" by 20" and was located one chord behind the trailing edge of the airfoil. The chord Reynolds numbers tested were 1×10^6 and 2×10^6. The model wake was surveyed at airfoil angles of attack of 0°, 2°, 4°, 6°, 8° and 10°.

In order to investigate the effect of the turbulence intensity on profile drag measurement, a 1" diameter cylinder was tested at a Reynolds numbers of 50,000 and 100,000. The survey planes (Fig. 5b) for the cylinder were located 8 and 12 diameters downstream from the center of the cylinder.

A single component hot wire was used to determine the streamwise turbulence intensity. The hot wire was oriented in endflow with the sensor wire such that it was sensitive to flow in the xy plane. Data were taken for 5 seconds at a sample rate of 2000Hz. Three pressure probes, a 7-hole probe, a chamfered total probe and a $\cos^2$ probe were used to determine the total and static pressures, and the flow angularity. The three pressure probes were all 0.125" in diameter. The $\cos^2$ or Rossow probe was made following the analysis of Rossow[10] in order to obtain the cosine squared characteristics, i.e. $W_x = 0$. However, due to error in the manufacture, the W_x of this probe was approximately 0.6. The center hole of the 7-hole probe was sensitive to the flow angularity where the W_x was close to 0. During the test, two probes could be mounted simultaneously on the strut that was positioned by the 2-D traverse system.

DATA REDUCTION

The drag coefficient was calculated in this paper using van Dam's equation (Eq. 8), Jones' equation (Eq. 10), and the simplified Jones' equation (Eq. 11) for comparison. The drag coefficients presented have all been corrected for the effects of solid body blockage and wake blockage according to Rae and Pope's analysis.[15] In order to study the effect of wake turbulence, total pressures with and without correction were used in the calculations.

Only a single component of the turbulence in the xy plane was measured in our test. When the three components of the turbulence were required, they were estimated using the assumptions below based on prior experimental data and known probe characteristics.

S809 airfoil

In order to correct for the effects of the turbulence on the readings of the probes, the following assumptions were made according to Coles and Wadcock's[13] result that the two components of the turbulence in the x-z plane are equal.

1) $w_{rms}^2 = u_{rms}^2$, and $v' = 0$ assuming 2-D flow. The results obtained based on this assumption were indicated by 'corr1'.

2) The turbulence in all three directions are isotropic, thus $u_{rms}^2 = v_{rms}^2 = w_{rms}^2$. The results obtained based on this assumption were indicated by 'corr2'.

Cylinder

Based on Cantwell and Coles[13], at the center of the wake and 8-diameters downstream, $(u_{rms}^2/U_\infty^2)_{max} \cong 0.045$ and $(w_{rms}^2/U_\infty^2)_{max} \cong 0.052$ and as the distance downstream increased the two components tended to be equal. Based on this, the following assumptions were made:

1) $w_{rms}^2 = 1.2u_{rms}^2$ at the 8-diameter downstream location
   $w_{rms}^2 = u_{rms}^2$ at the 12-diameter downstream location
   We also assume that the wake is exactly 2-D and then $v' = 0$.

The results obtained according to these assumptions were marked by 'corr1'.

However, we know that the flow is not be 2-D. Hence, another set of assumptions was also used. By assuming that the turbulence in the y-z plane, the plane perpendicular to the x-axis, is isotropic and considering the results of Cantwell and Coles[13], we assume:

2) $v_{rms}^2 = w_{rms}^2 = 1.2u_{rms}^2$ at the 8-diameter downstream location
   $u_{rms}^2 = v_{rms}^2 = w_{rms}^2$ at the 12-diameter downstream location.

The results obtained according to these assumptions were marked by 'corr2'.

Total Pressure Correction

The turbulence components were determined from the hot-wire data and the appropriate assumption. The total pressure from the different probes was corrected according to Eqs. (13, 14, and 15) and the assumptions above. Due to error in the manufacture the Rossow ($\cos^2$) probe did not follow Eq. (14). Instead Eq. (15) was used with an experimentally determined W_x of 0.6.

RESULTS AND DISCUSSION

Cylinder

In order to validate the wake survey method for the highly turbulent wake of the airfoil with simulated ice, the wake of a 1" diameter cylinder was investigated in detail. Figures 6 - 8 give the field distributions of the normalized total pressure, static pressures and streamwise turbulence intensity at Re = 50,000. The data are for the planes normal to the flow located at 8 diameters (8D) and 12 diameters (12D) downstream from the center of the cylinder. The total and static pressures were determined using the 7-hole probe and are shown uncorrected for the effect of turbulence. The streamwise turbulence intensity was determined using the single component hotwire and assuming $v' = 0$. It can been seen that the wake of the cylinder was wide and the static pressure in the wake was far below the static pressure of the freestream. Similar results can be found in Takahashi's test[3]. With the large loss in static pressure seen in Fig. 7 the contribution of the pressure term on the total drag in Eq. (8) will be large.

Figure 9 shows the streamwise turbulence intensity distribution across the wake at the midspan of the cylinder at 8D and 12D downstream and Re = 50,000. The steamwise turbulence intensity was determined using the single component hotwire (also assuming $v' = 0$). It was found when comparing these measurements to those of Cantwell and Coles[13] that they were significantly lower. Cantwell and Coles found wake turbulence intensities 8D downstream and at a Re = 140,000 of approximately 21% compared to the 12 – 14% seen here. In investigating these discrepancies it was discovered that the low-pass filter used during the hot-wire measurements was incorrectly set to 300Hz, thus artificially reducing the measured turbulence intensity. To correct for this, the current measured results were scaled using Cantwell and Coles results and those are the corrected results plotted in Fig. 9.

The total pressure distribution at the midspan of the cylinder with/without turbulence correction 8D and 12D downstream at Re = 100,000 is shown in Fig. 10. The notation 7HP, cos^2 and PIT represent the 7-hole probe, $\cos^2$ probe and chamfered Pitot probe, respectively. The total pressure was corrected according to case 2, as described previously. The discrepancy in the measurements was reduced significantly after correcting for the turbulence effects.

Figure 11 plots the contribution of the three terms in Eq. (8) on the total drag coefficient for three cases. As the measurements moved downstream to the 12D location the pressure contribution decreased and the momentum component increased. The total drag coefficient value was also reduced in closer agreement to the value of 1.237 reported by Cantwell and Coles.[13] Note also the negative contribution from the Reynolds stress term in Eq. (8) due to the minus sign that originates in the normal shear stress from Eq. (6).

Figure 12 shows the drag coefficients calculated using van Dam's equation (Eq. 8) and the simplified Jones' equation (Eq. 11). The data from the three probes', with and without turbulence correction were used to calculate the drag coefficient. It can be seen that although there are differences between the results using the uncorrected total pressure data from the different probes, they become very close after correction for the turbulence effects. In particular, except for the 7-hole probe all the drag coefficient values are closer to the assumed correct value of 1.237 and the corrections significantly reduce the difference in the values from the different probes showing that their different sensitivities to the turbulence is indeed being corrected. Table 1 give the actual drag coefficient values and the differences from the 1.237 value.

Table 2 gives the drag coefficient results generated from the three different equations using the 7-hole probe data with/without turbulence correction. It can be seen that the simplified Jones' equation (Eq. 11) works better than the original Jones' equation (Eq. 10). The van Dam equation also works well. It implies that the original Jones' equation may be not suitable for high turbulent wake.

The results (Table 2) also suggest that both the van Dam and simplified Jones' methods could give similar results if the 'true' total and static pressures were obtained. For example, according to the results of 'corr2' at Re = 100K, the average result of the simplified Jones' equation is 1.251 which is 1.1% larger than Contwell and Coles'[13] result of 1.237, the average result of van Dam's equation is 1.228 which is 0.8% lower than 1.237. However, van Dam's method is not convenient in experimental investigation due to the additional measurements required. The simplified Jones' method is preferred for the following reasons:

1) The static pressure, which is also affected by the turbulence and difficult to correct, is not required.
2) The u' term does not appear in Jones' equation although the u_{rms} may still be required to correct the total pressure measurements.

Table 1: Results calculated using simplified Jones' equation and data from various probes.

Location	Re (K)	Probe	Un-corr	Error %	Corr1	Error %	Corr2	Error %
8D	50	7HP	1.189	-3.9	1.247	0.8	1.247	0.8
		$\cos^2$	1.058	-14.5	1.168	-5.6	1.204	-2.7
		PIT	0.957	-22.6	1.113	-10.0	1.178	-4.8
	100	7HP	1.223	-1.1	1.265	2.3	1.265	2.3
		$\cos^2$	1.105	-10.7	1.191	-3.8	1.218	-1.5
		PIT	0.992	-19.8	1.110	-10.2	1.160	-6.3
12D	50	7HP	1.173	-5.2	1.232	-0.4	1.232	-0.4
		$\cos^2$	1.129	-8.7	1.227	-0.8	1.262	2.0
		PIT	1.058	-14.5	1.184	-4.3	1.245	0.7
	100	7HP	1.249	1.0	1.296	4.7	1.296	4.7
		$\cos^2$	1.161	-6.1	1.238	0.1	1.267	2.4
		PIT	1.086	-12.2	1.187	-4.1	1.236	-0.1

* 7HP --- 7-hole probe, $\cos^2$ --- $\cos^2$ probe, PIT --- chamfered Pitot probe.

It can be seen that the $\cos^2$ probe, which had good flow angularity sensitivity and are not sensitive to the cross streamwise turbulence components, are a good choice. Rossow[10] has studied these probes in detail. However, these probes have some disadvantages: 1) very difficult to manufacture, 2) sensitive to the alignment. The $\cos^2$ probe has the advantage, however, that it needs only the streamwise turbulence component to correct its total pressure measurement.

The chamfered Pitot tube is also a good choice for wake survey investigation because it can be handled relative easily, particularly with respect to alignment. However, it must be corrected in highly turbulent flow and all three turbulence components are needed, hence, the determination of the total turbulence kinetic energy, is critical.

Based on these findings it is clear that by correcting for the wake turbulence, excellent agreement to previously determined cylinder drag coefficient could be determined from wake measurements. This provides confidence that similarly good results can be obtained for highly separated iced airfoils. In these measurements only the simplified Jones equation will be used. The original Jones equation has been shown to be less accurate and the van Dam equation requires static pressures which are not always available.

Table 2: Results calculated using different equations.

Location	Re (K)	Method*	Un-corr	Error %	Corr1	Error %	Corr2	Error %
8D	50	v.D.	1.226	-0.9	1.304	5.4	1.304	5.4
		O.J.	1.430	15.6	1.485	20.0	1.457	17.8
		S.J.	1.189	-3.9	1.247	0.8	1.247	0.8
	100	v.D.	1.271	2.7	1.328	7.3	1.328	7.3
		O.J.	1.497	21.0	1.561	26.2	1.561	26.2
		S.J.	1.223	-1.1	1.265	2.3	1.265	2.3
12D	50	v.D.	1.187	-4.1	1.248	0.9	1.248	0.9
		O.J.	1.297	4.9	1.367	10.5	1.367	10.5
		S.J.	1.173	-5.2	1.232	-0.4	1.232	-0.4
	100	v.D.	1.230	-0.6	1.283	3.7	1.283	3.7
		O.J.	1.393	12.6	1.450	17.2	1.450	17.2
		S.J.	1.249	1.0	1.296	4.7	1.296	4.7

*: v.D. --- van Dam's equation, Eq(8),
O.J. --- Original Jones' equation, Eq(10),
S.J. --- Simplified Jones' equation, Eq.(11).

S809 AIRFOIL

Based on the analysis of the results for the cylinder, the simplified Jones' method was used in the S809 investigation. The turbulence effect was considered for some cases which have high turbulence intensity.

Clean Airfoil

Figures 13 - 17 show the field distributions of normalized total pressure, static pressure, flow angularity and streamwise turbulence intensity of the clean S809. The data were obtained from the 7-hole probe and the single component hot wire at three different angles of attack (0°, 4° and 8°) and Re = 1 million.

In the total pressure distribution (Fig. 13), the wake can be easily seen. The initially narrow wake at $\alpha = 0°$ grows rapidly and moves to a more negative z location as the angle of attack increased. It can be seen in Fig.14 that there is no obvious static pressure deficit in the wake. What was seen was a decrease in static pressure above the airfoil induced by the lift (circulation) as the velocity above the airfoil increased. Figures 15 and 16 show that the flow angularity in the wake is very small, usually less than 3°, for the angles of attack shown. The definition of the flow angles was

shown in Fig. 2. For airfoils with ice accretion the lifts are relatively small even near maximum lift, suggesting that the effects of flow angularity on the drag coefficient calculation can be neglected.

The streamwise turbulence intensity (u_{rms}/U_∞), Fig. 17, obtained using the single component hot wire and assuming $v' = 0$ is shown. The wake of S809 was very small compared to the cylinder wake, Fig. 8. The maximum (u_{rms}/U_∞) in the wake of the clean S809 was lower than 5% at 1 chord downstream, while the measured maximum (u_{rms}/U_∞) in the cylinder wake was approximately 15% at 8D downsteam.

In Fig. 18 the midspan distribution of total pressure obtained using three different pressure probes shows that, though the width of the wake grew with α, the maximum deficit of total pressure changed little as the angle of attack increased. It also can be seen that the results from the three pressure probes are almost the same even at large angle of attack (e.g. 8°). It suggests that the small turbulence intensity has almost no effect on the readings of the probes with different nose shapes. Hence, the turbulence effect on the total pressure was not considered for the clean S809 in the calculation of the drag coefficient.

Figure 19 gives the comparison of the drag coefficient results at the midspan of the S809 airfoil obtained from the data from the different probes. All of the results are within a few drag counts and show that the nose shape of the probe was not critical in these low-turbulence wakes.

S809 with Simulated Ice

Figures 20 - 22 give the field distribution of normalized total pressure, static pressure and streamwise turbulence intensity at the 1 chord downstream location of the S809 airfoil with simulated ice. Data are shown at three angles of attack (0°, 4° and 8°) and Re = 1M. The total pressure wake deficit (Fig.20) is seen to occur over a much larger z distance and represent a larger loss in total pressure as compared to the clean airfoil data in Fig. 13. This is as expected due to the large drag caused by the ice simulation. Unlike the clean case, an obvious deficit of static pressure in the wake can be seen at large angle of attack (Fig. 21). According to Fig. 22c, the streamwise turbulence distribution at 8° angle of attack, the wake from the upper surface was very unsteady at high angle of attack. Turbulence intensities approaching 16% were measured in this unsteady separated flow induced by the simulated ice. Again the low-pass filter was set at 300Hz, so actual turbulence intensities were probably somewhat larger.

The midspan distribution of the turbulence intensity in the wake of the iced S809 is shown in Fig. 23 for the 3 highest α's tested. It can be seen that the turbulence became very high when the angle of attack was greater than 6°, and at 10° angle of attack the turbulence intensity was even higher than that measured behind the cylinder (Fig. 9). Therefore, the turbulence effect on the measured total pressure must be considered and the corrected total pressure should be used in the calculation of the drag coefficient.

Figure 24 gives the comparison of the cross-wake distribution of the total pressures for the iced S809 airfoil obtained from the three different probes with/without turbulence correction at two angles of attack (6° and 10°). The total pressure was corrected according to the assumption that the turbulence was isotropic (case 2: $u_{rms} = v_{rms} = w_{rms}$ where u_{rms} was determined from the hot wire assuming $u_{rms} = v_{rms}$). At α = 6° the measurements from all three probes, with/without correction, were essentially identical. Here u_{rms}/U_∞ at the wake center was approximately 8%. At α = 10° the Pitot and the Rossow probe measured lower total pressure in the center of the wake where the turbulence intensity was high (over 18% from Fig. 23). In Fig. 24(d) the turbulence corrections decreased the total pressures measured by the Pitot and Rossow probes (and to a lesser extent the 7-hole probe) bringing them into better agreement. Based on more detailed analysis, this suggests that the effect of turbulence on total pressure measurement could be ignored when the maximum turbulence intensity (u_{rms}/U_∞) was less than 8%.

The drag coefficient at angles of attack from 0 to 10 degrees is shown in Fig. 25. These were calculated using the simplified Jones' equation, data from the 3 probes, and the two different turbulence correction schemes. Only for α's of 6° and above have the turbulence corrections been applied. It can be seen that, after corrected according to the turbulence effect, the three pressure probes give similar drag coefficients. Also note, if the turbulence intensity (u_{rms}/U_∞) was less than 8% (iced S809 at 6° angle of attack), the change of drag coefficient with/without correction was less than 3% (Table 3). It suggests that the turbulence effect can be neglected when the turbulence intensity is less than 8%.

The results in Table 3 show that correcting for the turbulence intensity reduced the difference in the Cd's calculated from the three probes, but they do not agree as well as the cylinder data. This is probably due to the low turbulence values obtained from the hot wire. In

each case the Pitot probe result was much lower than the other two. Since the Pitot probe is the most sensitive to increased measured total pressure and, therefore, reduced C_d due to turbulence, it is clear that a higher measured turbulence would improve the calculated drag coefficients.

Table 3: Results of Iced S809 at Large Angle of Attack.

AoA	Correction	7-hole probe	$\cos^2$ probe	Pitot probe	$\Delta C_d / \overline{C}_d$
6°	uncorr	0.0582	0.0576	0.0576	1%
	corr1	0.0593	0.0592	0.0598	1%
	corr2	0.0587	0.0588	0.0592	0.85%
8°	uncorr	0.1127	0.1086	0.1050	7.1%
	corr1	0.1170	0.1162	0.1138	2.9%
	corr2	0.1149	0.1140	0.1116	2.9%
10°	uncorr	0.1875	0.1782	0.1653	12.5%
	corr1	0.1956	0.1930	0.1826	6.8%
	corr2	0.1916	0.1893	0.1783	7.1%

CONCLUSIONS

This preliminary study considered how accurately the drag coefficient of a cylinder and airfoil with a highly separated unsteady wake could be determined using the wake survey method. Based on this research, the following conclusions can be made:

1. The cylinder and iced airfoil wakes were highly turbulent and affected the measured wake total pressures from the 3 probes according to the probe tip geometry.
2. The measured wake streamwise total pressures from the three probes used could be brought into good agreement by knowing the probe turbulence characteristics and the three turbulence components.
3. The cylinder drag coefficient could be measured to within 5% of the assumed correct value using the corrected total pressures and the simplified Jones equation or the van Dam equation, which included the turbulent stress term.
4. Flow angles in the wake were low (< 3 degrees) and for the iced airfoil where maximum lift is low the flow angle can be ignored.
5. An accurate drag coefficient for an iced airfoil should be obtainable from the wake survey method using simple probes for total pressure and wake turbulence measurement and standard momentum integral equations.
6. More research is needed in iced airfoil wakes to understand the turbulence field to enable the total pressure measurements to be accurately corrected.
7. Further validation of the iced airfoil case is required, but results from this study are very encouraging.

ACKNOWLEDGEMENT

This work was supported by the National Aeronautics and Space Administration (NASA) under grant NAG 3-1988. The authors would like to thank Mr. Gene Addy, Mr. Tom Bond, Dr. Mark Potapczuk and Dr. Judy van Zante from NASA Glenn for their contributions to this research.

REFERENCES

[1] Betz, A., "A Method for the Direct Determination of Wing Section Drag," NACA TM 337, 1925.

[2] Jones, B. M., "Measurement of Profile Drag by the Pitot-Traverse Method," British ARC R&M 1688, 1936.

[3] Takahashi, T. T., "On the Decomposition of Drag from Wake Survey Measurements," AIAA 97-0717, 1997.

[4] Goett, Harry. J., "Experimental Investigation of The Momentum Method for Determining Profile Drag," Report No. 660, Langley Memorial Laboratory, 1939.

[5] Antonia, R. A. and Rajagopalan, S., "Determination of Drag of a Circular Cylinder," AIAA Journal, Vol. 28, No. 10, 1990, pp.1833-1834.

[6] Chao, D. D and van Dam, C. P., "Airfoil Drag Prediction and Decomposition," Journal of Aircraft, Vol. 36, No. 4, 1999, pp. 675-681.

[7] van Dam, C. P., "Recent Experience with Different Methods of Drag Prediction," Progress in Aerospace Sciences 35, 1999, pp. 751-798.

[8] Goldstein, S., "A Note on the Measurement of Total Head and Static Pressure in a Turbulent Stream," Proceedings of the Royal Society of London, Series A, Vol. 155, 1936, pp. 570-575.

[9] Becker, H. A. and Brown, A. P. G., "Response of Pitot Probes in Turbulent Streams," J. Fluid Mech., Vol. 62, Part 1, 1974, pp. 85-114.

[10] Rossow, Vernon J., "Probe Shapes for Streamwise Momentum and Cross-Stream Turbulence Intensity," J. of Aircraft, Vol. 28, No. 11, 1991, pp. 741-749.

[11] Rossow, Vernon J., "Probe Systems for Static Pressure and Cross-Stream Turbulence Intensity," J. of Aircraft, Vol. 28, No. 11, 1991, pp. 750-755.

[12] Coles, D. and Wadcock, Alan J., "Flying-Hot-Wire Study of Flow Past an NACA4412 Airfoil at Maximum Lift," AIAA Journal, Vol. 17, No. 4, 1979, pp. 321-329.

[13] Cantwell, B. and Coles, D., "An Experimental Study of Entrainment and Transport in the Turbulent Near Wake of a Circular Cylinder," J. Fluid Mech., Vol. 136, 1983, pp. 321-374.

[14] Schlichting, H., "Boundary-Layer Theory," 7th edition, New York, McGraw-Hill, 1969.

[15] Rae, W. H. and Pope, A., "Low-Speed Wind Tunnel Testing," 2nd edition, John Wiley & Sons, 1984.

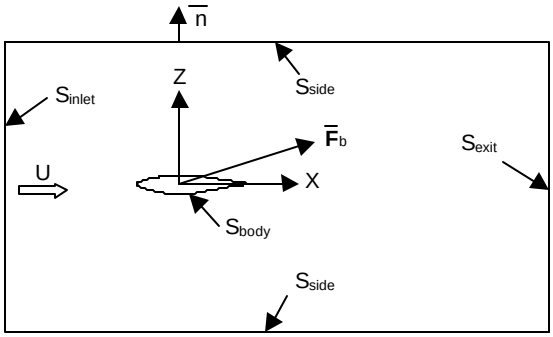

Fig. 1 Schematic of Body in Uniform Flow Inside Control Volume ($S = S_{exit} + S_{side} + S_{inlet}$)

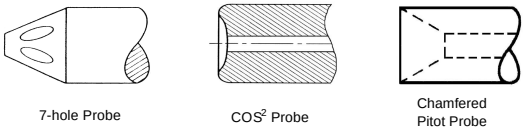

Fig. 2 Schematic of the Nose Shape of the Probes.

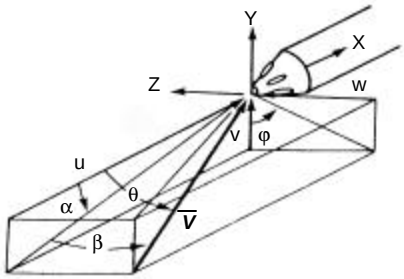

Fig. 3 Flow Angle Definitions.

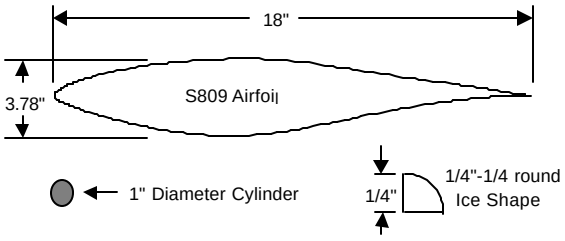

Fig. 4 Schematic of S809, ¼"-¼"-Round Ice Shape and 1" Diameter Cylinder Used in the Test.

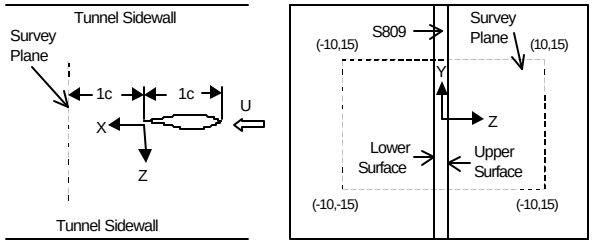

(a) Survey Plane for S809 Airfoil

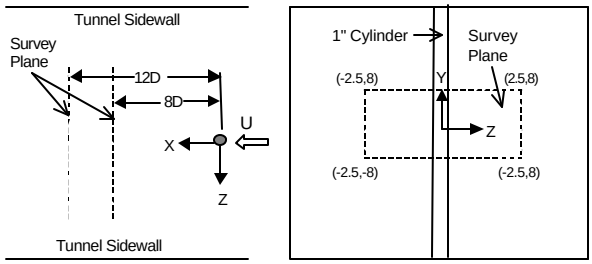

(b) Survey Plane for the Cylinder

Fig. 5 Schematic of the Survey Plane.

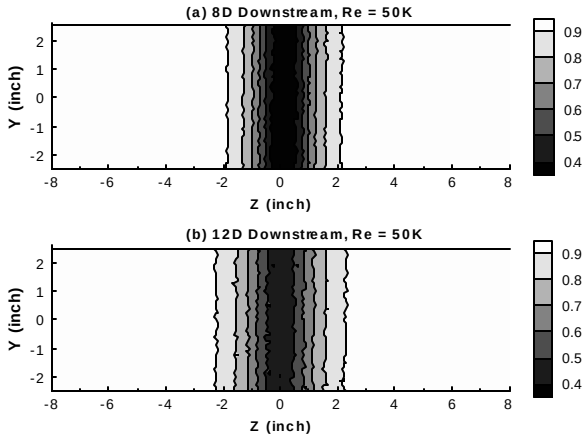

Fig. 6 Normalized Measured Total Pressure [$(p_{t,w} - p_{s,\infty})/q_\infty$] Contour of the Cylinder Wake at Re =50K.

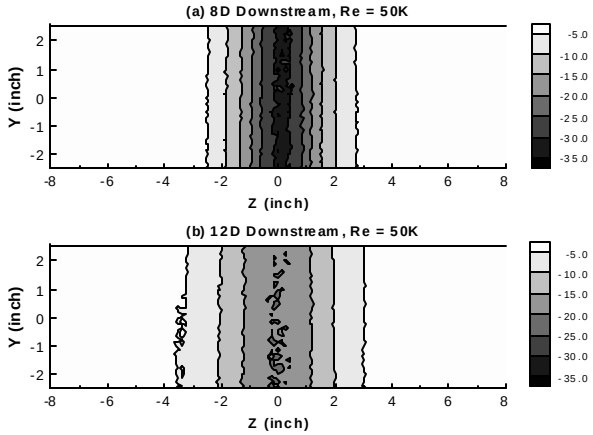

Fig. 7 Normalized Measured Static Pressure [$(p_{s,w} - p_{s,¥})/q_{¥}\times100$] Contour of the Cylinder Wake at Re =50K.

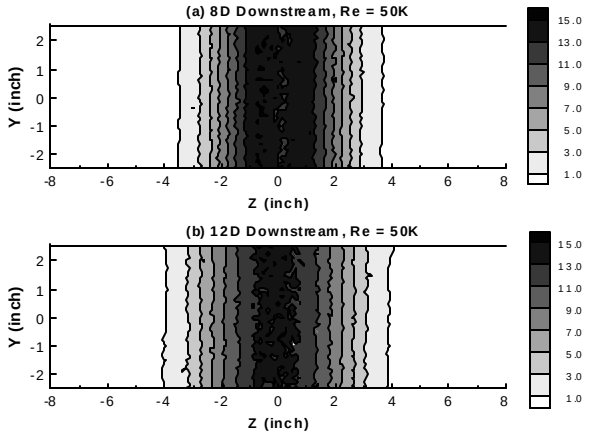

Fig. 8 Measured Turbulence Intensity [$u_{rms}/\ U_{¥}\times100$] Contour of the Cylinder Wake at Re=50K.

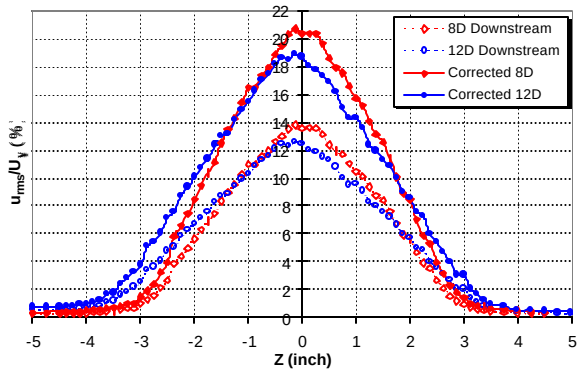

Fig. 9 Streamwise Turbulence Intensity (with/ without correction) Distribution across the Wake of the 1" Diameter Cylinder (Re = 100K).

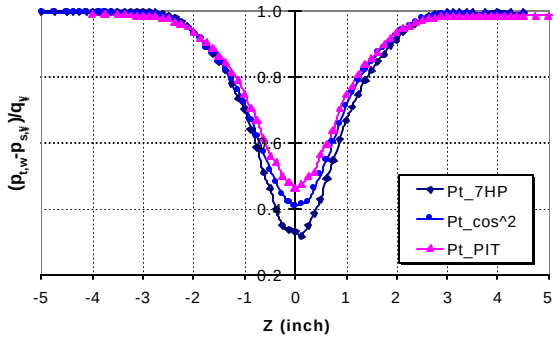

(a) 8D Downstream, without correction

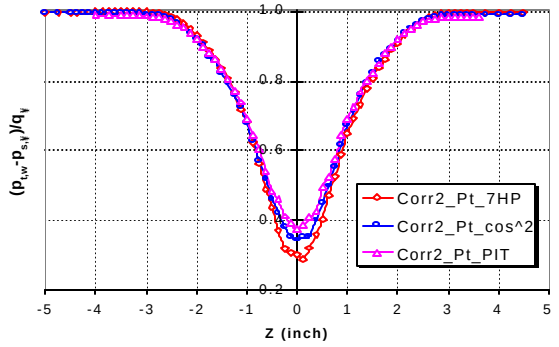

(b) 8D Downstream, with correction

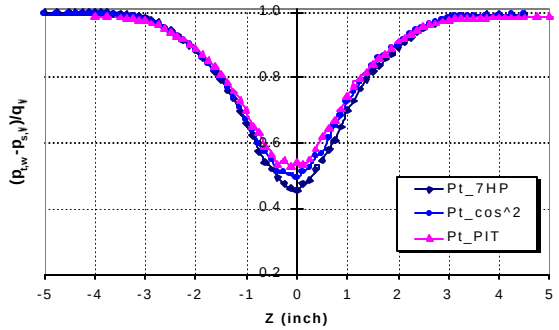

(c) 12D Downstream, without correction

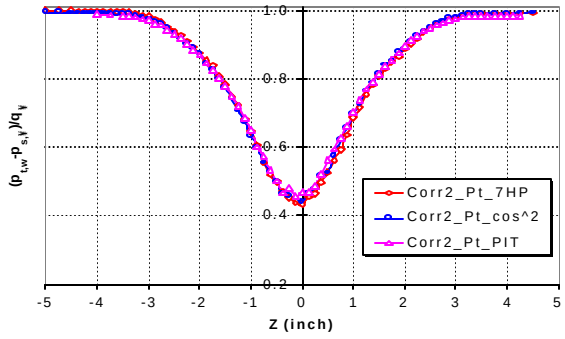

(d) 12D Downstream, wth correction

Fig. 10 Comparison of the Normalized Total Pressure Distribution (with/without Correction) of the Cylinder Wake (Re=100K).

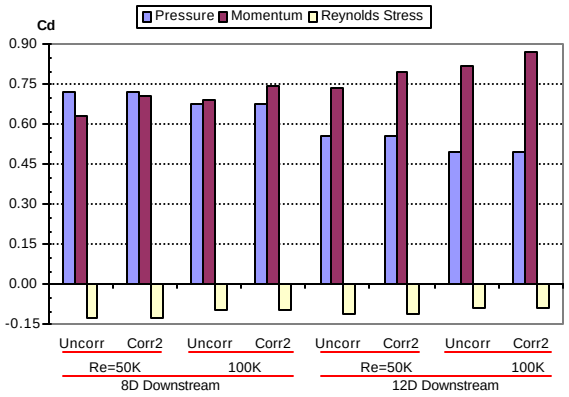

Fig. 11 Contributions of the Three Components on the Total Drag Coefficient

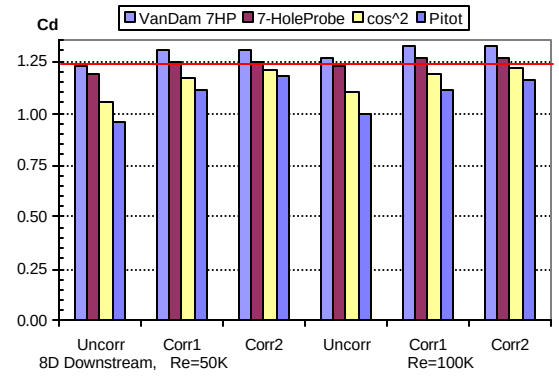

(a) Results of 8D Downstream Location

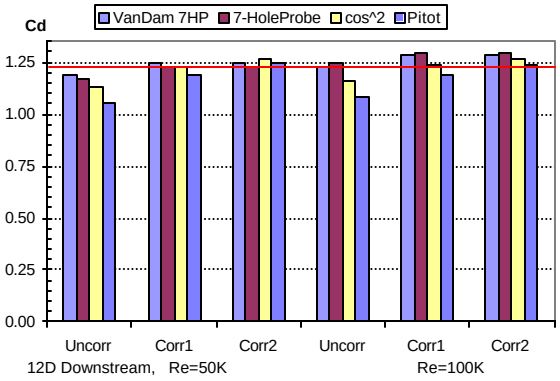

(b) Results of 12D Downstream Location

Note: 'VanDam 7HP' means the Cd is calculated using Van Dam method and the data of 7-hole probe, the others Cds are calculated using Jones' method. 'Uncorr' and 'Corr1' & 'Corr2' represent the total pressure is uncorrected or corrected according to the turbulence effect based on different assumptions. Solid line refers the result of 1.237.

Fig. 12 Drag Coefficient of the Cylinder Obtained by Different Methods and Data.

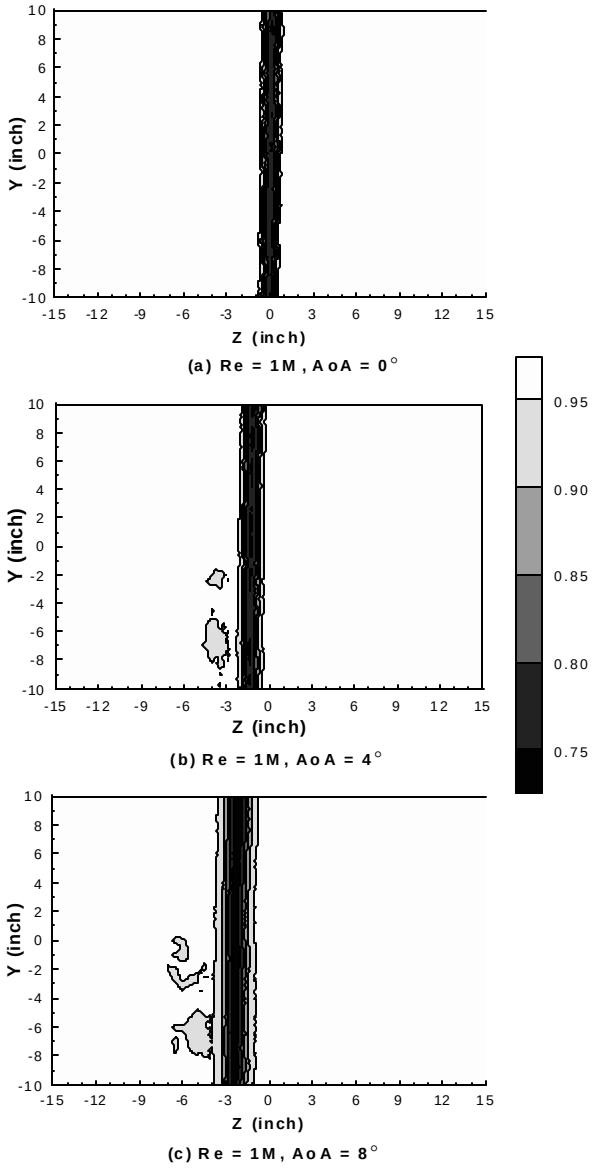

Fig. 13 Normalized Measured Total Pressure $[(p_{t,w} - p_{s,\infty})/q_\infty]$ Distribution in the of Clean S809 Wake.

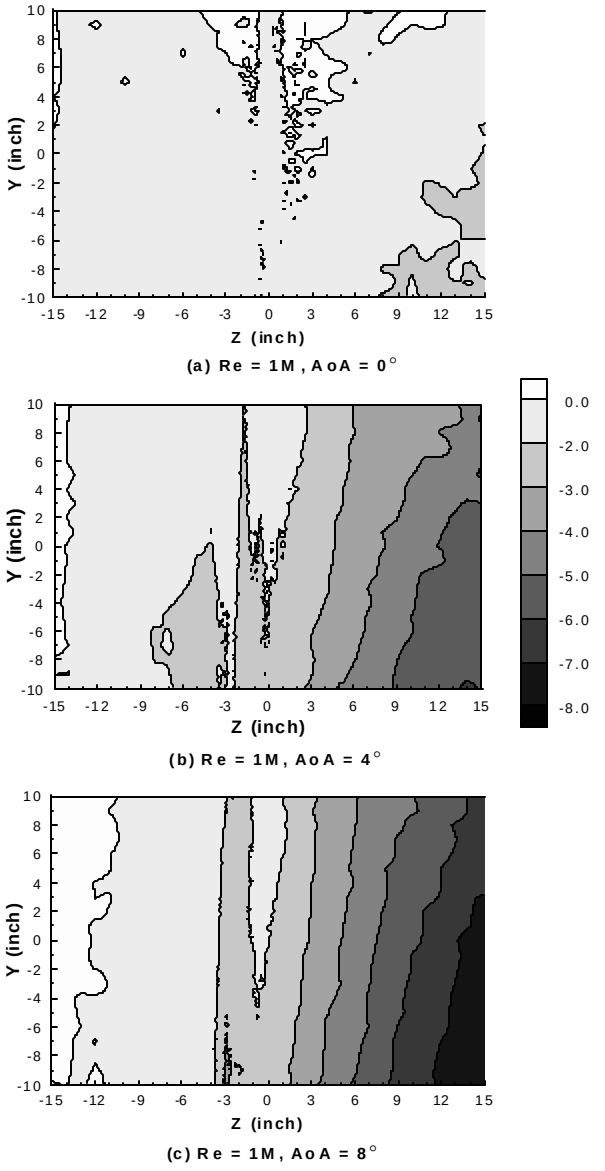

Fig. 14 Normalized Measured Static Pressure [$(p_{s,w} - p_{s,\infty})/q_\infty \times 100$] Distribution in the Clean S809 Wake.

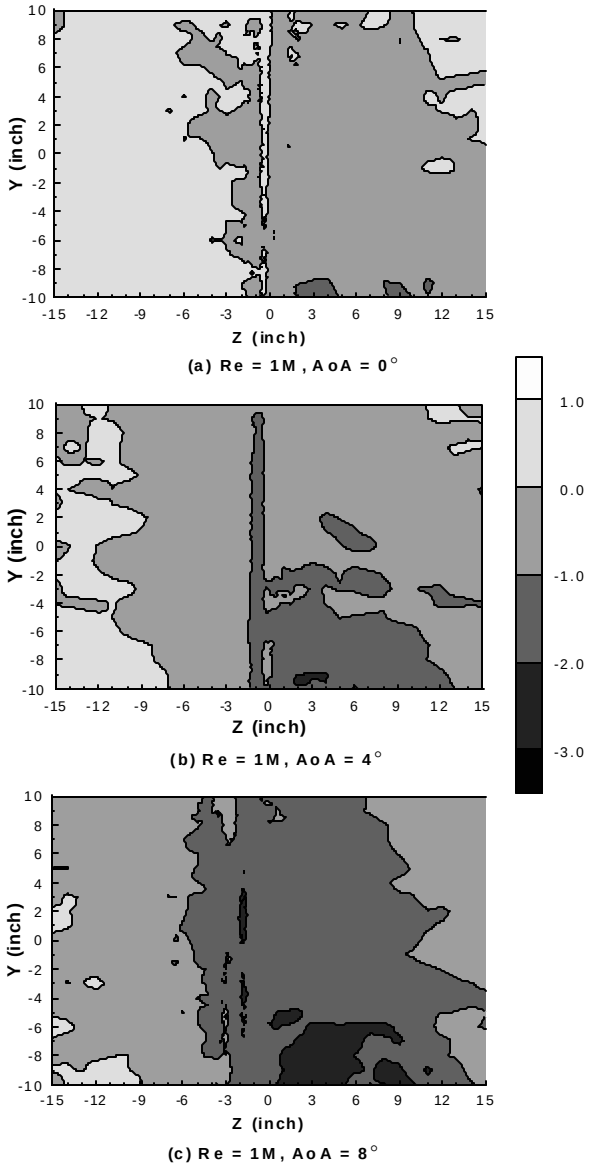

Fig. 15 Cross-Stream Plane Distribution of Flow Angle, α (deg.), in the Clean S809 Wake.

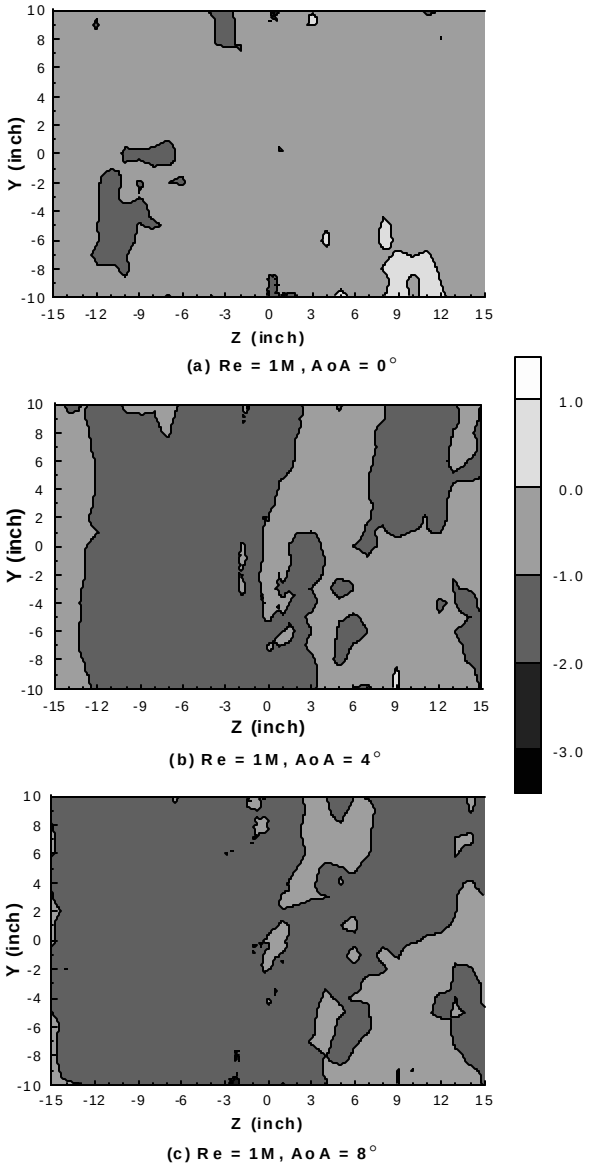

Fig. 16 Cross-Stream Plane Distribution of Flow Angle, β (deg.) in the Clean S809 Wake.

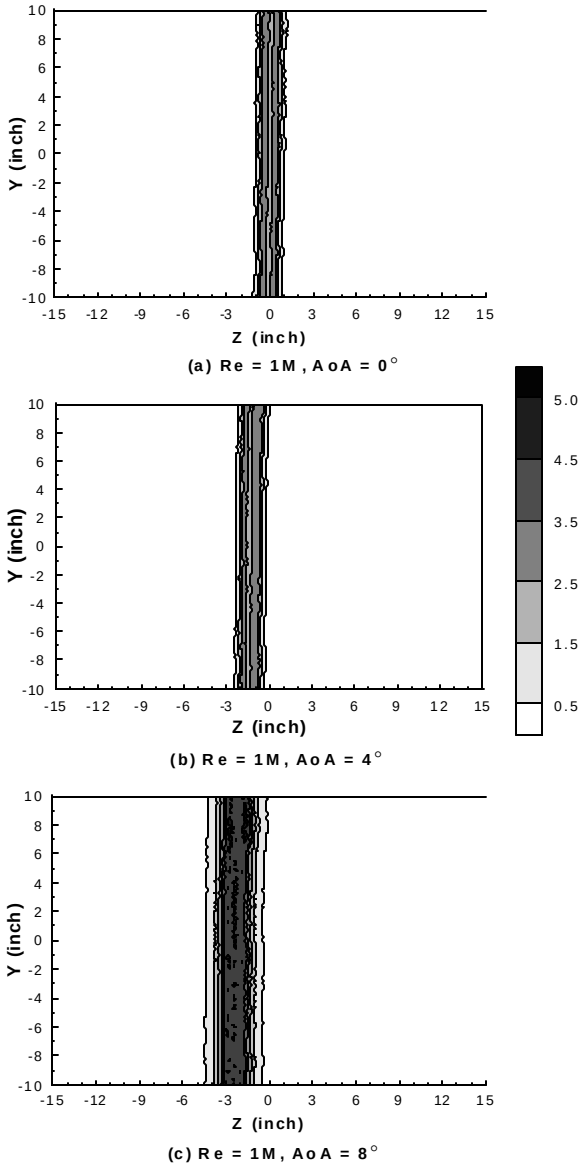

Fig. 17 Measured Streamwise Turbulence Intensity $[u_{rms}/U_{\infty}\times 100]$ Distribution in the Cross-Stream Plane of the Clean S809 Wake.

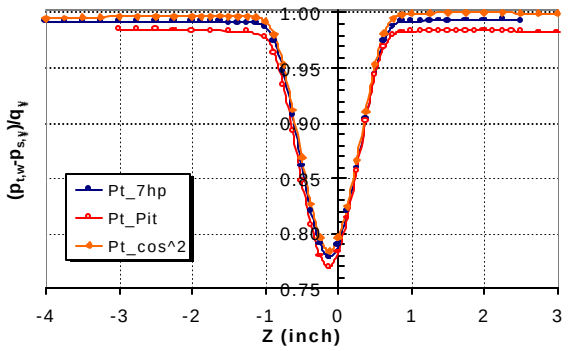

(a) Re = 1M, AoA = 0°

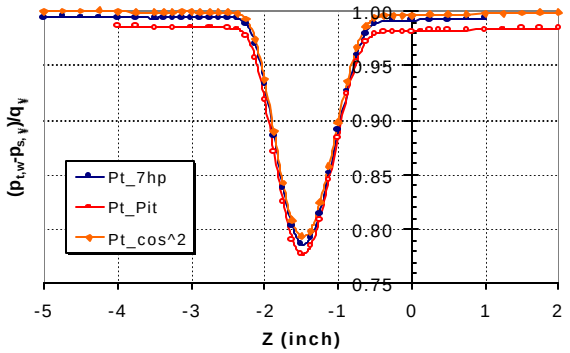

(b) Re = 1M, AoA = 4°

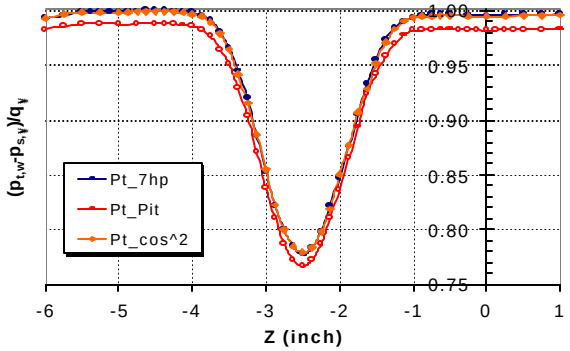

(c) Re = 1M, AoA = 8°

Fig. 18 Normalized Measured Wake Total Pressure $[(p_{t,w} - p_{s,¥})/q_¥]$ Distribution at Midspan of the Clean S809.

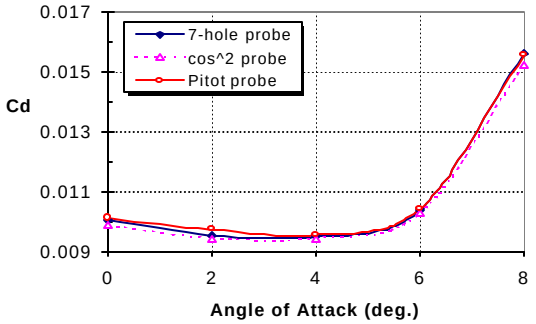

Fig. 19 Results of Drag Coefficient of Clean S809 Calculated from Different Probes' Data (Re=1M).

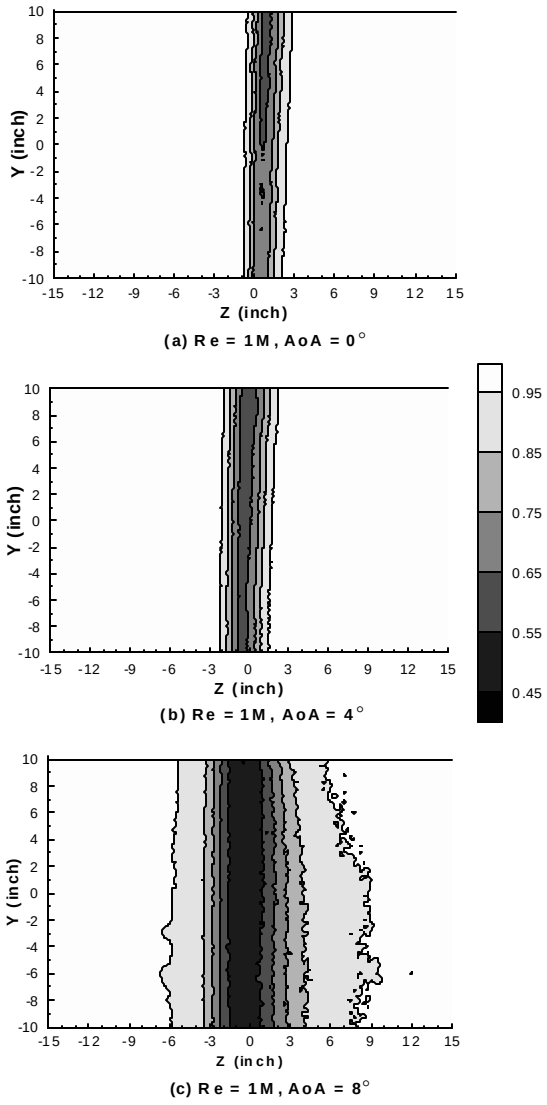

Fig. 20 Normalized Measured Wake Total Pressure $[(p_{t,w} - p_{s,¥})/q_¥]$ Distribution of the S809 with L.E. Ice.

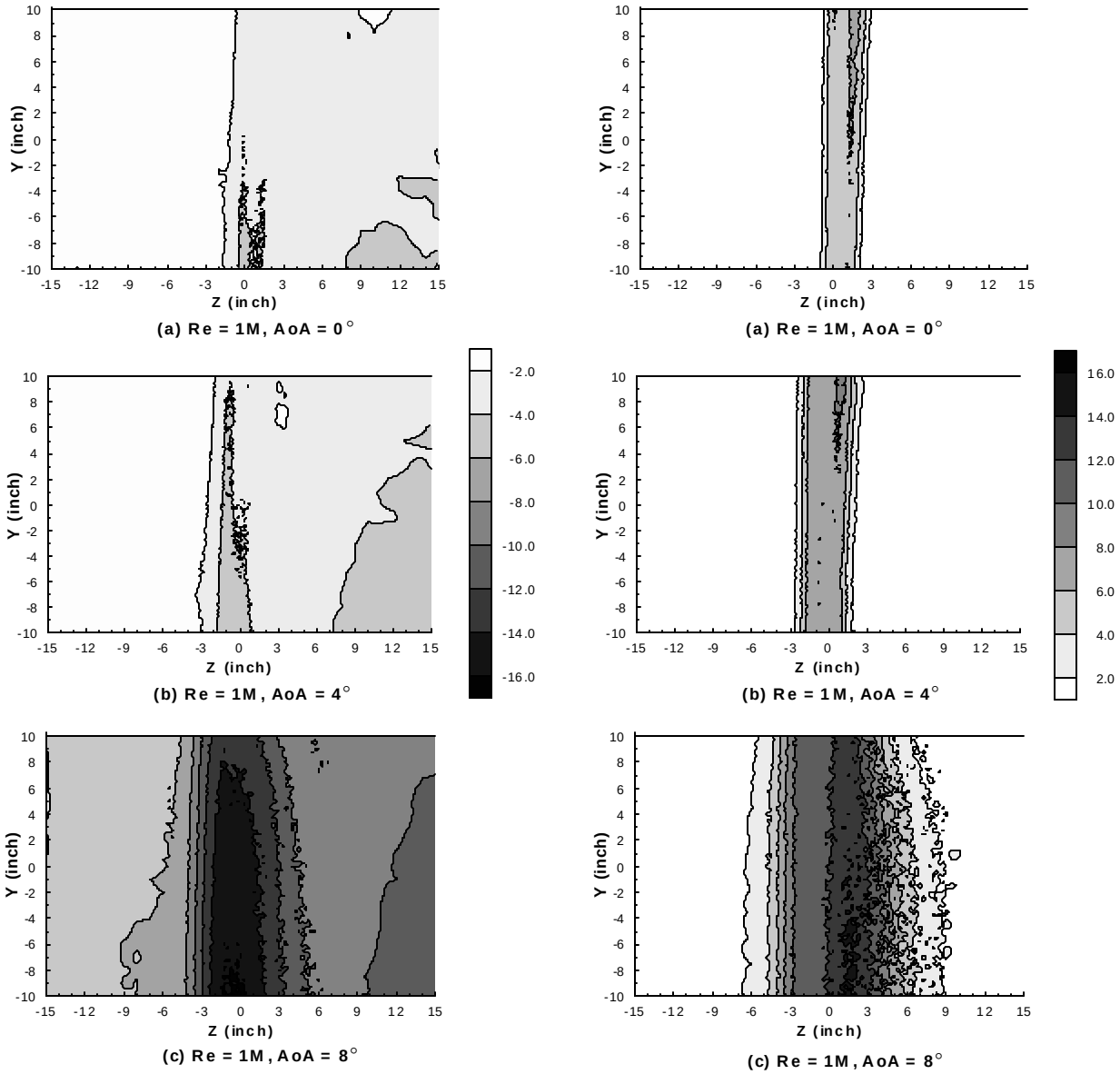

Fig. 21 Normalized Measured Wake Static Pressure $[(p_{s,w} - p_{s,¥})/q_{¥} \times 100]$ Distribution of the S809 with L.E. Ice.

Fig. 22 Measured Wake Streamwise Turbulence Intensity $[u_{rms}/U_{¥} \times 100]$ Distribution at the Cross Streamwise Plane for the S809 with L.E. Ice.

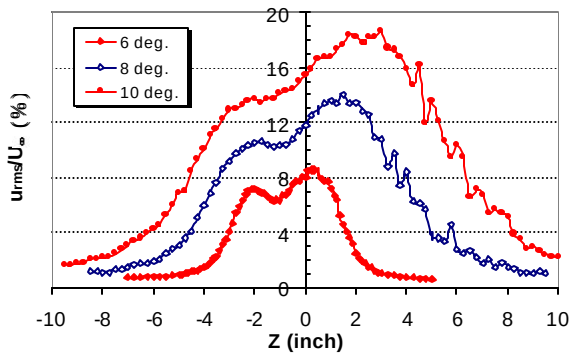

Fig. 23 Streamwise Turbulence Intensity [$u_{rms}/U_{¥}$ ×100] Distribution across the Wake of the S809 with L.E. Ice at Large Angles of Attack.

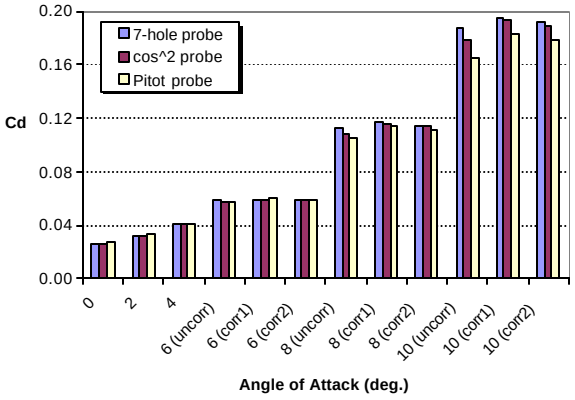

Fig. 25 Results of Drag Coefficient Calculated using the Simplified Jones' Equation and Different Probes' Data with/without Corrections for the S809 with L.E. Ice at Re = 1M.

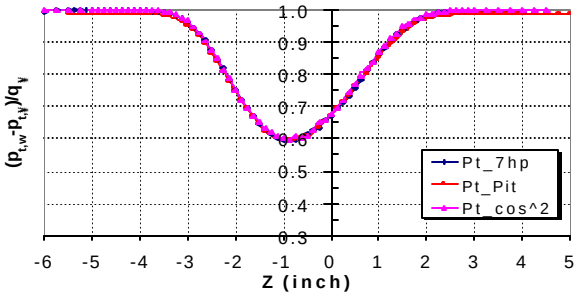

(a) Re = 1M, AoA = 6°, without correction

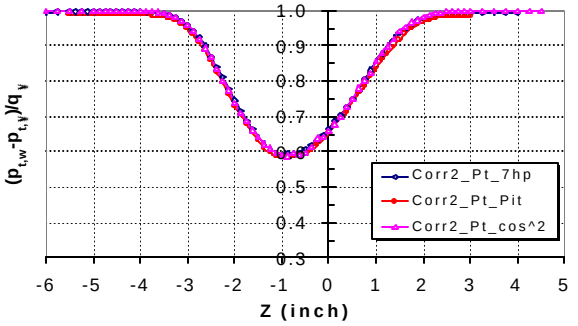

(b) Re = 1M, AoA = 6°, with correction

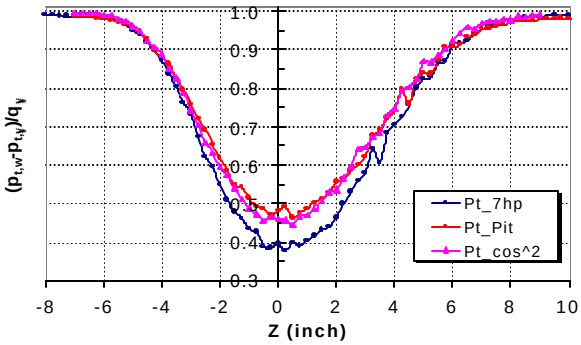

(c) Re = 1M, AoA = 10°, without correction

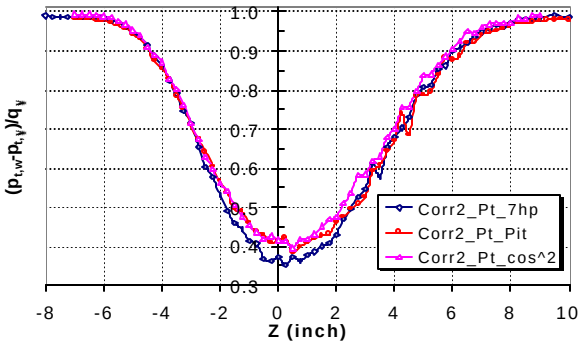

(d) Re = 1M, AoA = 10°, with correction

Fig. 24 Distribution of Wake Total Pressure (with and without correction) at the Midspan of the S809 with L.E. Ice.